

## Physicochemical Characterization of Tamoxifen Citrate Pseudopolymorphs, Methanolate and Ethanolate

Takashi KOJIMA,\*<sup>a</sup> Fumie KATO,<sup>a</sup> Reiko TERAOKA,<sup>a</sup> Yoshihisa MATSUDA,<sup>a</sup> Shuji KITAGAWA,<sup>a</sup> and Mitsutomo TSUHAKE<sup>b</sup>

<sup>a</sup> Department of Pharmaceutical Technology, Kobe Pharmaceutical University; and <sup>b</sup> Department of Functional Molecular Chemistry, Kobe Pharmaceutical University; Higashi-Nada, Kobe 658–8558, Japan.

Received October 4, 2006; accepted December 15, 2006; published online December 20, 2006

Two novel pseudopolymorphs, methanolate and ethanolate of tamoxifen [(*Z*)-2-[4-(1,2-diphenyl-1-butenyl)phenoxy]-*N,N*-dimethylethylamine]citrate, were prepared in addition to forms A and B reported previously. Their crystalline forms were identified and characterized by powder and single crystal X-ray diffractometry, differential scanning calorimetry, thermogravimetric analysis, hot-stage microscopy, scanning electron microscopy and diffuse reflectance infrared Fourier-transform spectroscopy, and their physicochemical stability was also evaluated. The results of single crystal X-ray analysis and thermogravimetric analysis of methanolate and ethanolate suggested that the stoichiometry of tamoxifen citrate : methanol and tamoxifen citrate : ethanol could be composed of a 1 : 1 molecular ratio for both solvates. The results of physicochemical stability evaluations at 75 and 97% RH at 40 and 60 °C indicated that the metastable form A was quite stable for at least 2 months even under severe storage conditions, whereas methanolate immediately transformed to a crystalline mixture of forms A and B, and subsequently changed to the stable form B.

**Key words** tamoxifen; pseudopolymorph; physicochemical characterization; physicochemical stability

During the development process of solid drugs, the most desirable crystal form should be appropriately selected based on the information of physicochemical properties including polymorphism, their salt<sup>1,2)</sup> and co-crystal formation<sup>3)</sup> of drug candidates, because physicochemical properties can affect efficacy, safety,<sup>4–6)</sup> stability,<sup>7,8)</sup> manufacturing process<sup>9,10)</sup> and quality control.<sup>11)</sup> Recently, understanding the polymorphism has been positioned as an important research, since polymorphs and pseudopolymorphs show different physicochemical properties<sup>7,8,12–18)</sup> including solubility.<sup>6)</sup> Generally, a stable polymorph shows low solubility and high stability, and metastable polymorphs exhibit higher solubility and lower stability. From the viewpoint of the manufacturing process, information about organic solvates is also valuable for the selection of a crystallization solvent. Appropriate selection of the crystalline form from polymorphs and pseudopolymorphs should be conducted in order to achieve the purposes of development; this contributes to the improvement of stability, bioavailability and manufacturability.

Tamoxifen, (*Z*)-2-[4-(1,2-diphenyl-1-butenyl)phenoxy]-*N,N*-dimethylethylamine, is one of the selective estrogen receptor modulators and tamoxifen citrate is widely used as a drug for the treatment of breast cancer. Tamoxifen has also been used as a model pharmaceutical compound for preformulation studies and several researches have been conducted.<sup>2,19–23)</sup> As for tamoxifen citrate (Fig. 1), two polymorphs, forms A and B, were identified.<sup>24)</sup> Previously, we have investigated the photostability of forms A and B, and

discussed the difference in photostability from the viewpoint of solid-state UV/Vis absorption spectroscopy.<sup>25)</sup> Even though tamoxifen citrate is widely used throughout the world, detailed characterization of its polymorphs and pseudopolymorphs has not been reported to the best of our knowledge.

In this study, we prepared two novel pseudopolymorphs, methanolate and ethanolate, in addition to forms A and B reported previously. Their crystal forms were identified and characterized by powder and single crystal X-ray diffractometry, differential scanning calorimetry (DSC), thermogravimetric analysis (TGA), hot-stage microscopy, scanning electron microscopy (SEM) and diffuse reflectance infrared Fourier-transform spectroscopy (DRIFTS), and their physicochemical stability was also evaluated.

### Experimental

**Preparation of Modifications** Tamoxifen citrate was obtained from EGIS Pharmaceuticals (Budapest, Hungary). All solvents were purchased from Wako Pure Chemical Industries (Osaka, Japan). Form A was bulk powder purchased from EGIS Pharmaceuticals. A small amount of form A for SEM observation was obtained by recrystallizing from saturated acetonitrile solution of the drug by seeding a small amount of bulk powder. Form B was obtained by recrystallizing from saturated isopropyl alcoholic solution of the drug with stirring overnight at room temperature. Form B was then filtrated and dried *in vacuo* at room temperature. Methanolate and ethanolate were obtained by recrystallizing from saturated methanolic and ethanolic solutions of the drug with stirring overnight at room temperature, respectively. Methanolate and ethanolate were then filtrated and dried in a nitrogen atmosphere.

**Scanning Electron Microscopy** Scanning electron micrographs were taken on a scanning electron microscope (JSM-5200LV, JEOL, Tokyo, Japan) at magnifications of 200–1000×. All powder samples were coated with thin gold film in an ion-sputter coater (JFC-1100, JEOL).

**Powder and Single Crystal X-Ray Diffractometries** Powder X-ray diffraction patterns were recorded using a RINT Ultima (Rigaku, Tokyo, Japan) with CuK $\alpha$  radiation generated at 30 kV and 14 mA at room temperature. Data were collected within diffraction angles from 2–40° (2 $\theta$ ) at a step size of 0.02° and a scanning speed of 4°/min.

Single crystal X-ray diffraction data were recorded on a SMART APEX II CCD X-ray diffractometer (Bruker AXS, Madison, WI, U.S.A.) with a Mo anode source at 90 K. The crystal structures were solved and refined using SHELXTL software.

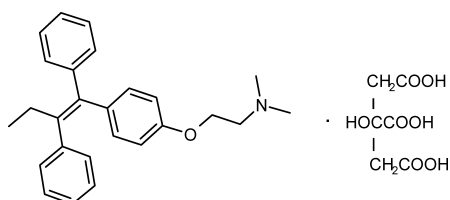


Fig. 1. Chemical Structure of Tamoxifen Citrate

\* To whom correspondence should be addressed. e-mail: tak\_kojimajpn@yahoo.co.jp

**Thermal Analysis** DSC was performed using a DSC 6200 system (Seiko Instruments, Chiba, Japan). A DSC thermogram was obtained in an aluminum open-pan system using a sample weight of ca. 3 mg and a heating rate of 5 °C/min under a nitrogen flow. TGA was performed using a TG/DTA 6200 system (Seiko Instruments). A TGA thermogram was obtained under the same conditions as those for DSC.

Thermal changes of crystal morphology were observed on a hot-stage microscope (LK-FDCS, Linkam Scientific Instruments, Surrey, U.K.) with a heating rate of 10 °C/min in a nitrogen flow.

**Diffuse Reflectance Infrared Fourier-Transform Spectroscopy** The FT-IR spectra of tamoxifen citrate polymorphs were recorded on a Spectrum One, Fourier-transform IR spectrometer (Perkin-Elmer, Wellesley, MA, U.S.A.) with diffuse reflectance after dispersion with KBr at room temperature. The samples were diluted with KBr to give 5% (w/w) mixture. A total of 64 scans was collected on each sample with 8 cm<sup>-1</sup> resolution. The spectra obtained were transformed to the Kubelka–Munk function unit for standardization.

**Physicochemical Stability** The physicochemical stability of forms A and B, methanolate, and ethanolate was evaluated by storing each ca. 500 mg of the sample at 75 and 97% RH at 40 and 60 °C in desiccators. Samples were removed after 3, 7, 14, 28 and 56 d and the crystal forms were evaluated by PXRD, DSC and TGA. Storage conditions were adjusted with saturated aqueous solutions of NaCl (75% RH) and K<sub>2</sub>SO<sub>4</sub> (97% RH).

## Results and Discussion

**Crystal Morphology** Morphological differences among crystal forms were observed using scanning electron microscopy (SEM) (Fig. 2). Form A crystals had a spindly needle shape, whereas form B crystals had a column shape. The appearances of methanolate and ethanolate crystals were similar and they were composed of needle-like agglomerates and were far smaller than form B crystals.

### Powder X-Ray and Single Crystal Diffraction Analyses

Powder X-ray diffraction (PXRD) patterns of crystal forms are shown in Fig. 3. The characteristic diffraction peaks of form A were observed at 2.9, 9.4, 11.6 and 13.8° (2θ), while those of form B were observed at 5.6, 12.7, 17.1 and 24.0° (2θ). Thus, significant differences between forms A and B were observed and PXRD patterns agreed well with the data reported previously.<sup>24</sup> The characteristic X-ray diffraction peaks of methanolate were observed at 4.9, 9.7, 14.2 and 21.6° (2θ), while those of ethanolate were observed at 4.7, 9.5, 13.9 and 21.4° (2θ), showing slight shifts to lower diffraction angles. Thus, methanolate and ethanolate showed quite similar PXRD patterns with 0.2°-shift. The crystal structures of form B, methanolate and ethanolate were analyzed by single crystal X-ray diffractometry. The results indicated that form B crystals (size=0.11×0.08×0.03 mm) were monoclinic ( $a=15.881(3)$ ,  $b=22.048(5)$ ,  $c=8.4701(18)$  Å,  $\beta=95.427(3)^\circ$ ), space group  $P2_1/c$  ( $Z=4$ , density=1.268 g/cm<sup>3</sup>,  $R_1=0.0537$ ), which coincided with the data reported already.<sup>24</sup> Methanolate (size=0.14×0.03×0.01 mm) and ethanolate (size=0.17×0.03×0.01 mm) were also monoclinic ( $a=10.612(5)$ ,  $b=16.479(8)$ ,  $c=36.35(2)$  Å,  $\beta=94.164(12)^\circ$ ) and space group  $P2_1/n$  ( $Z=4$ , density=1.246 g/cm<sup>3</sup>,  $R_1=0.1008$ ), and monoclinic ( $a=10.639(2)$ ,  $b=16.512(3)$ ,  $c=36.707(8)$  Å,  $\beta=93.108(6)^\circ$ ) and space group  $P2_1/n$  ( $Z=4$ , density=1.258 g/cm<sup>3</sup>,  $R_1=0.0981$ ), respectively. The results of single crystal analysis of methanolate and ethanolate also clearly indicated that arrangements of tamoxifen and citric acid molecules in the crystal were similar and the stoichiometry of tamoxifen citrate : methanol and tamoxifen citrate : ethanol was confirmed to be a 1 : 1 molecular ratio for any solvate (Fig. 4a). Hydrogen bonds between alcohol molecule and terminal carboxylic

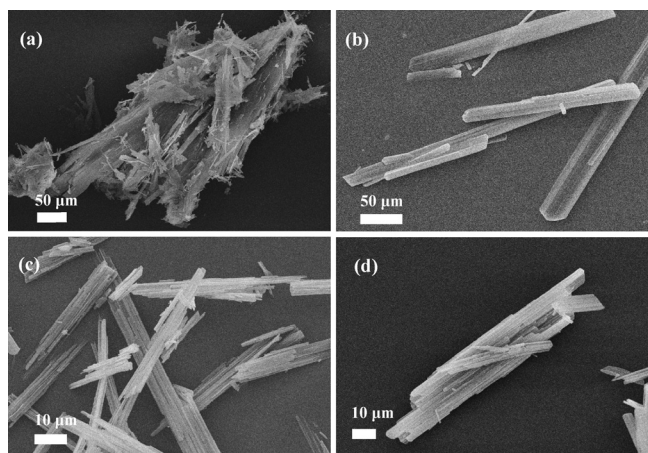


Fig. 2. Scanning Electron Photographs of Tamoxifen Citrate Modifications

(a) Form A; (b) form B; (c) methanolate; (d) ethanolate.

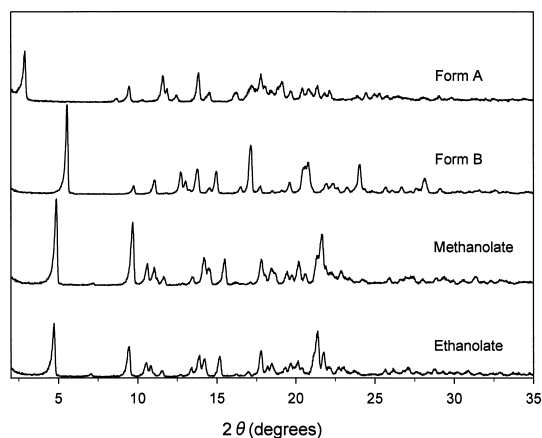


Fig. 3. PXRD Patterns of Forms A and B, Methanolate and Ethanolate

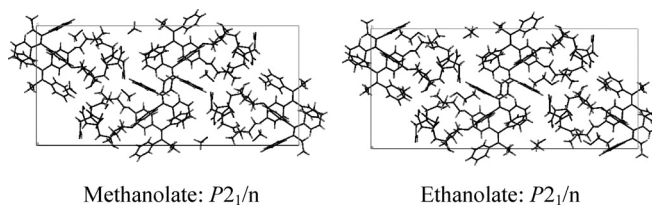


Fig. 4a. Crystal Structures of Methanolate and Ethanolate

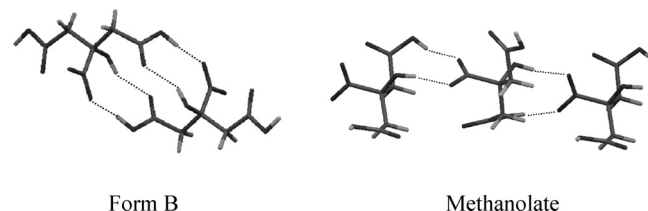


Fig. 4b. Cyclic Pairs of Hydrogen Bonding of Citrate Species in Form B and Methanolate Crystals

function of citric acid molecule were observed and resulted in differences of intermolecular interaction between adjacent citrate species compared with form B crystals in which a 9-membered circle hydrogen bond was formed (Fig. 4b).<sup>24</sup> However, a single crystal of form A, of sufficient size for sin-

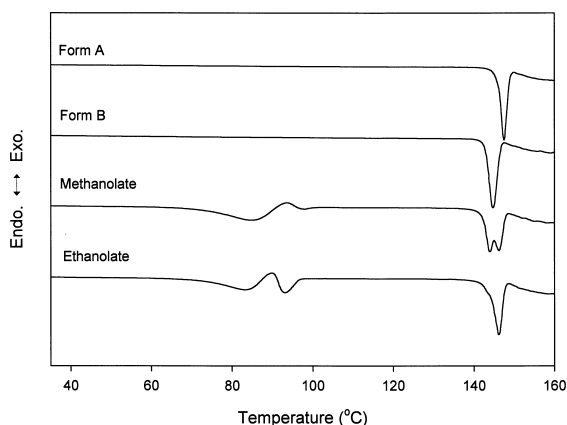


Fig. 5. DSC Thermograms of Forms A and B, Methanolate and Ethanolate

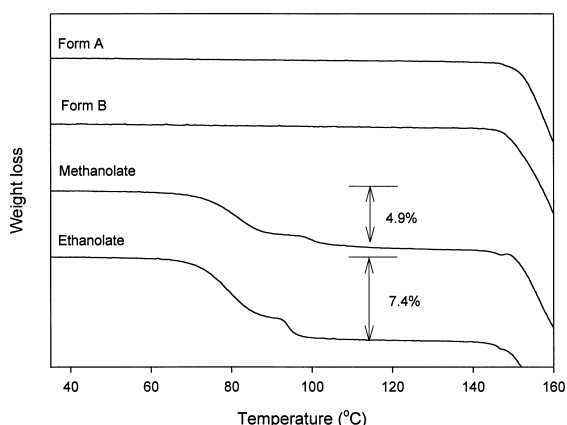


Fig. 6. TGA Thermograms of Forms A and B, Methanolate and Ethanolate

gle crystal X-ray analysis, could not be obtained, even though crystallization was extensively attempted under various conditions.

**Thermal Properties** DSC curves of forms A and B showed melting endothermic peaks at 147.5 and 144.8 °C, respectively (Fig. 5). The heat of fusion ( $\Delta H_f$ ) of forms A and B was 59.7 and 63.7 kJ/mol, respectively, thus indicating that these forms have quite similar thermal properties. The DSC curve of methanolate seemed to show an endothermic peak at 85.7 and 98.1 °C, an exothermic peak at 94.1 °C, then two endothermic peaks at 144.2 and 146.5 °C, which corresponded with the melting points of forms B and A, respectively. The DSC curve of ethanolate also seemed to show two endothermic peaks at 84.1 and 94.0 °C, an exothermic peak at 90.4 °C, then two endothermic peaks at 143.5 and 146.3 °C, which corresponded with the melting points of forms B and A, respectively. The results of TGA thermograms of methanolate and ethanolate suggested that two-step desolvation of methanol and ethanol occurred, respectively (Fig. 6). Microscopic observation on the hot-stage proved that methanolate and ethanolate crystals melted slowly and crystallization occurred during the melting process (Figs. 7, 8). Taken together the results of DSC, TGA and hot-stage microscopy, both methanolate and ethanolate were melted with two-step desolvation and a mixture of forms A and B would be crystallized during the melting process. The peak

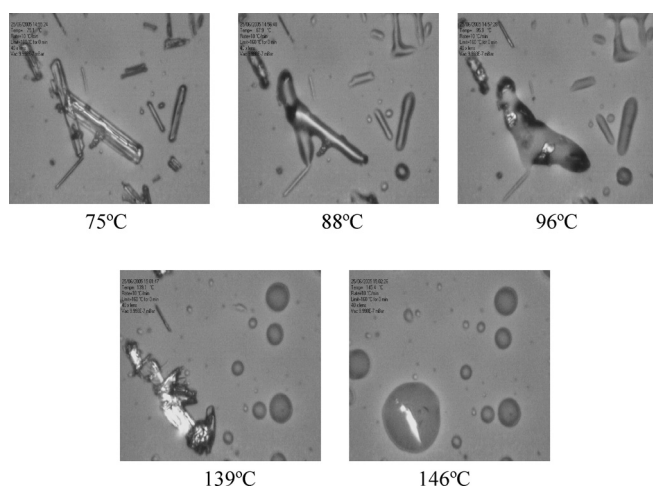


Fig. 7. Polarized Micrographs of Methanolate at Various Temperatures

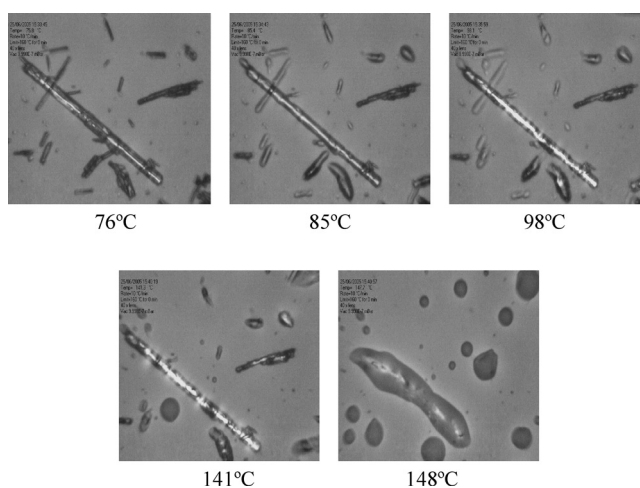


Fig. 8. Polarized Micrographs of Ethanolate at Various Temperatures

area ratio of the melting point of forms A to B on the DSC thermogram for methanolate was lower than that for ethanolate. Furthermore, the results of TGA thermograms of methanolate and ethanolate suggested that 4.9% of methanol and 7.4% of ethanol molecules were included in the crystal entity, respectively. The results of weight loss of these solvates stoichiometrically well corresponded with those of tamoxifen citrate monomethanolate and monoethanolate, which agreed well with the results of single crystal structure analysis.

It was previously reported that form A crystals suspended in ethanol transformed to form B.<sup>24)</sup> In their study, the existence of tamoxifen citrate ethanolate was not confirmed even though form A crystals were suspended in ethanol. Based on the results of our thermal analysis of ethanolate, form B crystals in the previous article reported by Goldberg<sup>24)</sup> would be observed after desolvation of ethanol from ethanolate and the subsequent transformation from the mixture of forms A and B to the stable form B.

**Spectroscopic Analysis** Tamoxifen citrate forms A and B, methanolate, and ethanolate were evaluated by diffuse reflectance infrared Fourier-transform spectroscopy (DRIFTS). In the FT-IR spectra, form A showed a sharp band at 1732  $\text{cm}^{-1}$  attributable to the stretching of C=O bond of cit-

ric acid, while form B showed a sharp band at  $3405\text{ cm}^{-1}$  attributable to the stretching of O–H bond and two strong bands at  $1707$  and  $1740\text{ cm}^{-1}$  attributable to C=O bond of citric acid (Fig. 9). Methanolate showed a broad band at  $3250\text{ cm}^{-1}$  attributable to O–H bond, and two strong bands at  $1720$  and  $1695\text{ cm}^{-1}$  attributable to C=O bond of citric acid. Ethanolate also showed a broad band at  $3243\text{ cm}^{-1}$  attributable to O–H bond, and two strong bands at  $1718$  and  $1697\text{ cm}^{-1}$  attributable to C=O bond of citric acid, thus indicating quite similar spectroscopic properties to methanolate. Based on the result of single crystal X-ray diffractometry, the O–H and C=O bonds of citric acid were involved in cyclic pairs of hydrogen bond interaction between adjacent citrate species. The differences of wave number in O–H and C=O bonds of citric acid between form B and solvate crystals were consistent with the result of crystal structures which showed different cyclic pairs of hydrogen bonding patterns.

**Physicochemical Stability of Polymorphs** The physicochemical stability of forms A and B, methanolate and ethanolate was evaluated at 75 and 97% RH at 40 and 60 °C, and the results are summarized in Table 1. Neither form A nor B transformed to each other even under these severe storage conditions, indicating that these forms were quite stable. This is consistent with the results shown in Fig. 5, where no thermal peak due to polymorphic transformation was observed for any of these forms. Methanolate immediately transformed to a crystalline mixture of forms A and B, and

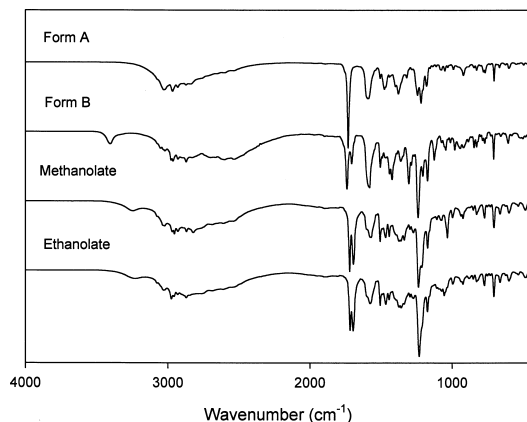


Fig. 9. FT-IR Spectra of Forms A and B, Methanolate and Ethanolate

subsequently transformed to the stable form B. On the other hand, ethanolate also immediately transformed to the crystalline mixture of forms A and B but no subsequent transformation to the stable form B completely occurred. Taking account of the results of both stability and DSC analysis, it could be said that the amount of stable form B in the crystalline mixture after desolvation of methanolate was more predominant than for ethanolate.

## Conclusion

We have provided for the first time a novel insight into tamoxifen citrate pseudopolymorphs, methanolate and ethanolate. Single crystal X-ray analysis and TGA revealed that the stoichiometry of tamoxifen citrate : methanol and tamoxifen citrate : ethanol was 1 : 1 in any case. The crystal structures of methanolate and ethanolate also revealed that intermolecular interaction between adjacent citrate species was different from that of form B crystals.

We have also demonstrated the physicochemical stability of crystal forms. Form A was quite stable for at least 2 months, whereas methanolate immediately transformed to the crystalline mixture of forms A and B after desolvation, and then changed to the stable form B.

Our investigation on the physicochemical properties of tamoxifen citrate methanolate and ethanolate would also provide useful information for the manufacturing process such as crystallization and drying process, and storage condition of tamoxifen citrate as active pharmaceutical ingredient.

**Acknowledgement** We wish to thank Dr. Kenji Yoza, Bruker AXS for single crystal X-ray analysis.

## References

- Gould P. L., *Int. J. Pharm.*, **33**, 201–217 (1986).
- Kojima T., Onoue S., Murase N., Katoh F., Mano T., Matsuda Y., *Pharm. Res.*, **23**, 806–812 (2006).
- Vishweshwar P., McMahon J. A., Bis J. A., Zaworotko M. J., *J. Pharm. Sci.*, **95**, 499–516 (2006).
- Aguiar A. J., Krc J., Jr., Kinkel A. W., Samyn J. C., *J. Pharm. Sci.*, **56**, 847–853 (1967).
- Poole J. W., Owen G., Silverio J., Freyhof J. N., Rosenman S. B., *Curr. Ther. Res. Clin. Exp.*, **10**, 292–303 (1968).
- Pudipeddi M., Serajuddin A. T., *J. Pharm. Sci.*, **94**, 929–939 (2005).
- Matsuda Y., Tatsumi E., *Int. J. Pharm.*, **60**, 11–26 (1990).
- Kato F., Otsuka M., Matsuda Y., *Int. J. Pharm.*, **321**, 18–26 (2006).
- Otsuka M., Hasegawa H., Matsuda Y., *Chem. Pharm. Bull.*, **45**, 894–898 (1997).

Table 1. The Solid-State Stability of Tamoxifen Citrate Modifications under Various Storage Conditions

Crystal form	Storage condition	Period (d)					
		Initial	3	7	14	28	56
Form A (A)	40 °C/75, 97% RH	A	A	A	A	A	A
	60 °C/75, 97% RH	A	A	A	A	A	A
Form B (B)	40 °C/75, 97% RH	B	B	B	B	B	B
	60 °C/75, 97% RH	B	B	B	B	B	B
Methanolate (M)	40 °C/75% RH	M	A (B) <sup>a</sup>	A (B) <sup>a</sup>	A (B) <sup>a</sup>	A, B	B (A) <sup>b</sup>
	40 °C/97% RH	M	A (B) <sup>a</sup>	A (B) <sup>a</sup>	B (A) <sup>b</sup>	B (A) <sup>b</sup>	B
	60 °C/75% RH	M	B (A) <sup>b</sup>	B	—	—	—
	60 °C/97% RH	M	B (A) <sup>b</sup>	B	—	—	—
Ethanolate (E)	40 °C/75% RH	E	A (B, E) <sup>c</sup>	A (B) <sup>a</sup>	A (B) <sup>a</sup>	A (B) <sup>a</sup>	A (B) <sup>a</sup>
	40 °C/97% RH	E	A (B) <sup>a</sup>	A (B) <sup>a</sup>	A (B) <sup>a</sup>	A (B) <sup>a</sup>	A (B) <sup>a</sup>
	60 °C/75% RH	E	A (B) <sup>a</sup>	A (B) <sup>a</sup>	A (B) <sup>a</sup>	A (B) <sup>a</sup>	A (B) <sup>a</sup>
	60 °C/97% RH	E	A (B) <sup>a</sup>	A (B) <sup>a</sup>	A (B) <sup>a</sup>	A (B) <sup>a</sup>	A (B) <sup>a</sup>

a) Predominantly form A with slight form B. b) Predominantly form B with slight form A. c) Predominantly form A with slight form B and ethanolate.

- 10) Sun C., Grant D. J., *Pharm. Res.*, **18**, 274—280 (2001).
- 11) Yu L. X., Lionberger R. A., Raw A. S., D'Costa R., Wu H., Hussain A. S., *Adv. Drug Deliv. Rev.*, **56**, 349—369 (2004).
- 12) Otsuka M., Teraoka R., Matsuda Y., *Pharm. Res.*, **8**, 1066—1068 (1991).
- 13) Otsuka M., Onoe M., Matsuda Y., *Pharm. Res.*, **10**, 577—582 (1993).
- 14) Bergren M. S., Chao R. S., Meulman P. A., Sarver R. W., Lyster M. A., Havens J. L., Hawley M., *J. Pharm. Sci.*, **85**, 834—841 (1996).
- 15) Henwood S. Q., Liebenberg W., Tiedt L. R., Lötter A. P., Villiers M. M., *Drug Dev. Ind. Pharm.*, **27**, 1017—1030 (2001).
- 16) Maurin M. B., Vickery R. D., Rabel S. R., Rowe S. M., Everlof J. G., Nemeth G. A., Campbell G. C., Foris C. M., *J. Pharm. Sci.*, **91**, 2599—2604 (2002).
- 17) Yoshihashi Y., Yonemochi E., Terada K., *Pharm. Dev. Technol.*, **7**, 89—95 (2002).
- 18) Chawla G., Gupta P., Thilagavathi R., Chakraborti A. K., Bansal A. K., *Eur. J. Pharm. Sci.*, **20**, 305—317 (2003).
- 19) Brigger I., Chaminade P., Marsaud V., Appel M., Besnard M., Gurny R., Renoir M., Couvreur P., *Int. J. Pharm.*, **214**, 37—42 (2001).
- 20) Bhatia A., Kumar R., Katare O. P., *J. Pharm. Pharm. Sci.*, **7**, 252—259 (2004).
- 21) Ho S., Calder R. J., Thomas C. P., Heard C. M., *J. Pharm. Pharmacol.*, **56**, 1357—1364 (2004).
- 22) Zeisig R., Ruckerl D., Fichtner I., *Anticancer Drugs*, **15**, 707—714 (2004).
- 23) Shenoy D. B., Amiji M. M., *Int. J. Pharm.*, **293**, 261—270 (2005).
- 24) Goldberg I., Becker Y., *J. Pharm. Sci.*, **76**, 259—264 (1987).
- 25) Kojima T., Onoue S., Katoh F., Teraoka R., Matsuda Y., Kitagawa S., Tshako M., *Int. J. Pharm.*, in press.